Plasmonics
DOI 10.1007/s11468-016-0283-5

Fishbone-Like High-Efficiency Low-Pass Plasmonic Filter Based on Double-Layered Conformal Surface Plasmons

Liangliang Liu[1] · Zhuo Li[1,2] · Bingzheng Xu[1] · Jia Xu[1] · Chen Chen[1] · Changqing Gu[1]

Received: 28 January 2016 / Accepted: 31 May 2016

Abstract In this work, we report a fishbone-like high-efficiency low-pass plasmonic filter based on a double-layered conformal surface plasmon waveguide (CSPW) which consists of double-layered symmetrical metal gratings (SMGs) of fishbone shape. Efficient mode conversion between the quasi-transverse electromagnetic (TEM) waves in the microstrip line and the conformal surface plasmons (CSPs) on the double-layered CSPW is realized by using gradient double-layered SMGs and impedance matching technique. Experimental results of the transmission and reflection coefficients of the straight sample show excellent loss-pass performance and agree well with the numerical simulations. The curved samples exhibit low radiation loss when the double-layered CSPW is conformal or even bent thanks to the high confinement of CSPs. The proposed structure can find potential applications in integrating conventional circuits with CSPs devices at microwave and terahertz frequencies.

Keywords Double-layered conformal surface plasmons · Mode conversion · Fishbone shape metal gratings · Low-pass plasmonic filter

✉ Zhuo Li
lizhuo@nuaa.edu.cn

[1] Key Laboratory of Radar Imaging and Microwave Photonics, Ministry of Education, College of Electronic and Information Engineering, Nanjing University of Aeronautics and Astronautics, Nanjing, 211106, China

[2] State Key Laboratory of Millimeter Waves, Southeast University, Nanjing, 210096, China

Introduction

The so called spoof surface plasmon polaritons (SPPs) propagating on textured conducting surfaces at deep subwavelength scale in the microwave and terahertz (THz) frequencies have been proposed and verified in the past decade [1–3]. These spoof SPPs inherit most of the exotic features of natural SPPs [4–6] as confining electromagnetic fields in a deep subwavelength scale with high intensity to overcome the diffraction limit. More importantly, their physical characteristics can be engineered at will by tuning the geometrical parameters. Among these works, the conformal surface plasmons (CSPs) [6], which are formed by printing ultrathin corrugated metallic strips on a flexible dielectric film, are regarded as one of the most potential candidates in developing practical ultrathin planar circuitry for microwave and THz applications [7–16].

However, it is hard to operate the CSPs devices independently due to the difficulties in feeding and extracting signals efficiently in the conventional planar microwave circuits, which are mostly two-conductor transmission line structures. Recently, several interesting works have been reported to realize smooth transition between conventional planar transmission lines (such as coplanar waveguide [7–9], microstrip line [10–13], and slot line [14–16]) and spoof SPP devices. In addition, deep subwavelength corrugated metallic wires [17] and domino structures [18] are also investigated to realize similar conversions at microwave frequencies. However, most of the proposed spoof SPP devices are constructed by single-layered corrugated symmetrical or antisymmetrical grooves, which are difficult to be integrated with a microwave or THz active chip owing to the single-layered structure. In addition, the bottom ground for coupling electromagnetic (EM) energy to convert the

Published online: 14 June 2016

direction of the electric field from perpendicular to parallel to the strip [10] will also increase the design difficulties and lead to low transmission efficiency especially at lower frequencies. Thus, how to efficiently excite the CSPs propagating on a double-layered CSPW in broadband becomes very necessary.

In this work, we propose a fishbone-like high-efficiency low-pass plasmonic filter based on a double-layered CSPW which consists of a double-layered SMGs of fishbone shape. Efficient mode conversion between the quasi-TEM mode in the microstrip line and the CSPs on the fishbone-like double-layered CSPW is realized by a smooth bridge, which is composed of two-stage back-to-back transitions from microstrip line to double-layered parallel-strip line [19] and periodic fishbone-like double-layered SMGs in between. Excellent agreement between the simulation and experimental results on the reflection and transmission coefficients of straight and curved CSPWs validates our design. The proposed transition structure is of simple structure, high realizability, seamless connection, and integration with microwave devices and circuits, which can find potential applications in advanced integrated circuits at microwave and THz frequencies.

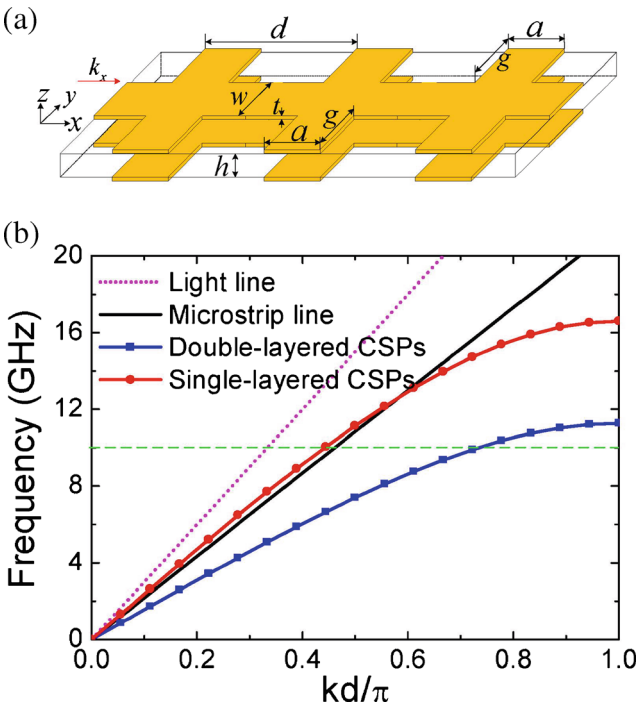

Fig. 1 The proposed double-layered CSPW with period d = 5 mm, width a = 1 mm along the x-axis and width w = 0.75 mm, length g = 2.1 mm along the y-axis, respectively. The top and bottom copper layers with the thickness t = 0.018 mm and separated by a dielectric substrate of Rogers RT5880 (ε_r = 2.2, tanδ = 0.0009) with the thickness h = 0.254 mm. **b** The dispersion relation for the fundamental surface mode of the single and double-layered CSPs

Model Analysis of Double-layered CSPs and Design of High Efficiency Low-pass Plasmonic Filter

The proposed double-layered CSPW has a fishbone shape shown in Fig. 1a, in which the period, length, and width of the double-layered SMGs are denoted by d, g, and a, respectively. In the microwave and THz frequencies, the metal can be reasonably assumed as perfect electric conductor (PEC). We are interested in calculating the dispersion relation of transverse magnetic (TM) polarized waves propagating in the x direction along the double-layered CSPW, and only the fundamental eigenmode is considered. As shown in Fig. 1b, the dispersion relations of the single- and double-layered SMGs are obtained by the eigenmode solver of the commercial software CST Microwave Studio [17, 18], in which the geometrical parameters are designed as d = 5 mm, g = 2.1 mm, a = 1 mm, t= 0.018 mm, and w = 0.75 mm, the dielectric substrate of thickness h = 0.254 mm is selected as Rogers RT5880 with relative dielectric constant ε_r = 2.2 and loss angle tangent tanδ = 0.0009. We observe that the dispersion curve of the double-layered symmetrical CSPs departs more from light line than that of the single-layered symmetrical CSPs and the cutoff frequency decreases significantly due to the enhanced equivalent capacitance and inductance by the strong EM coupling in the double-layered symmetrical structure. These unique properties result in a smaller propagating wavelength and bring tighter EM field confinement at the same frequency (see the green dotted line in Fig. 1b, λ=2π/k), holding promise for applications such as miniaturized CSPs devices and low crosstalk transmission lines.

In addition, we notice that there is a significant mismatch of momentum between the common microstrip line (see the dark line in Fig. 1b) and the double-layered CSPW (see the blue line in Fig. 1b), especially at the equivalent asymptotic frequency, which makes it difficult to excite double-layered CSPs propagating on this CSPW efficiently only by common microstrip line. To address it, a back-to-back matching transition with two stages from the microstrip line to a double-layered parallel-strip line and then to the double-layered CSPW is designed and shown as regions II and III in Fig. 3. Figure 2 illustrates the mode conversion theory explaining these two-stage conversions. Figure 2a shows that the dispersion curve is gradually deviating from the microstrip line and the cutoff frequency becomes lower when the length g increases from g_0 = 0 mm (g_0 = 0 mm represents the double-layered parallel-strip line) to g_7 = 2.1 mm step by step, which indicates higher confinement when g increases. Figure 2b shows that the normalized impedance changes from 1 to the impedance of the

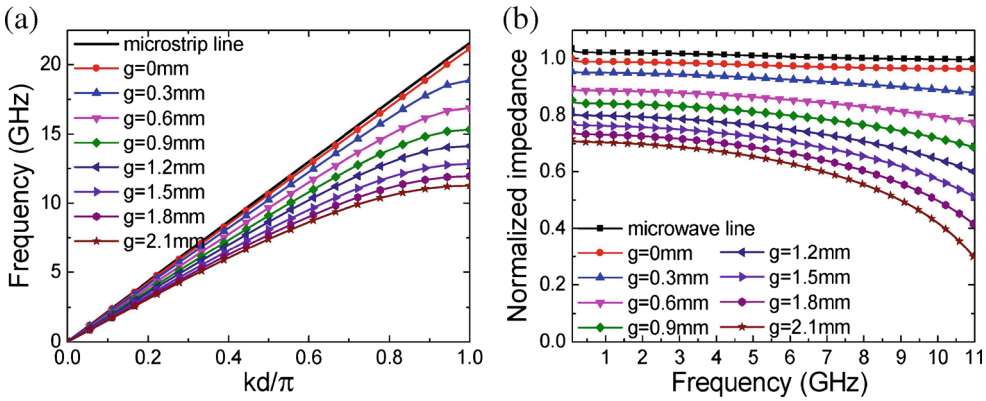

Fig. 2 The transition principle between the quasi-TEM waves and the double-layered CSPs with the length g of the periodic double-layered SMGs varying from 0 mm to 2.1 mm by a step of 0.3 mm, in which $g = 0$ mm represents the double-layered parallel-strip line. **a** and **b** are the evolution of the normalized wave vector and impedance respectively

double-layered CSPs, which is obtained using the S-parameter retrieval procedure [20]. Hence, the transition section functions as momentum and impedance matching between the microstrip line and double-layered CSPW simultaneously, thus facilitating the integration of the double-layered CSPs with traditional microwave devices and circuits.

By using two symmetrical transitions linked with a double-layered CSPW, we designed a high-efficiency low-pass plasmonic filter, which is typically composed of four regions with length $L_1 = 5$ mm, $L_2 = 17.5$ mm, $L_3 = 35$ mm, and $L_4 = 25$ mm along the x-axis shown in Fig. 3. Region I is a common microstrip line with signal line width $s = 0.75$ mm and ground width $T = 24$ mm. Region IV is the proposed double-layered CSPW with $d = 5$ mm, $a = 1$ mm, $w{=}s = 0.75$ mm, and $g = 2.1$ mm, respectively. The dielectric substrate can be designed and fabricated as ultrathin and flexible if needed and in our design h is chosen as 0.254 mm. Region II is the first-stage transition part with an inward flaring ground to realize smooth impedance matching from microstrip line to double-layered parallel-strip line, and the flaring curve is described as [17] $y{=}C_1e^{\alpha x} - C_2$ $(x_1 < x < x_2)$, with $\alpha = 0.2$, $C_1{=}(y_2 - y_1)/(e^{\alpha x_2} - e^{\alpha x_1})$, $C_2{=}(y_2e^{\alpha x_1} - y_1e^{\alpha x_2})/(e^{\alpha x_2} - e^{\alpha x_1})$, $p_1{=}(x_1, y_1)$ and $p_2{=}(x_2, y_2)$ being the start and end points of the flaring curve respectively. Note that the curve of the flaring ground can be designed differently. Region III is the second-stage transition part of a gradient double-layered SMGs with g varied from $g_1 = 0.3$ mm to $g_7 = 2.1$ mm with a step of 0.3 mm.

Results and Discussions

To evaluate the performance of the proposed design quantitatively, we fabricated a sample shown in Fig. 4a and measured its S-parameters (S_{11} is the reflection coefficient and S_{21} is the transmission coefficient) shown in Fig. 4c, in which all geometrical parameters keep the same as those in Fig. 3. In the experiment, Agilent N5230C vector network analyzer is employed and two coaxial cables with 50Ω port impedance are connected to both ends of the microstrip line via SMA connectors shown in Fig. 4a. Figure 4b illustrates the comparison of simulation results with and without the gradient matching gratings. If the transition part does not exist, we notice that the reflection coefficient (S_{11}) of the hybrid waveguide is higher than −4 dB from 6 to 10 GHz. That is to say, more than 40 % of the electromagnetic waves are reflected. With the matching transition, however, a very high-efficiency transmission is achieved, in which $S_{11}{<}{-}10$ dB, $S_{21}{>}{-}0.6$ dB in the frequency band from 0 to 10GHz. The measured S-parameters with the matching transition are demonstrated as the blue and magenta dotted lines in Fig. 4c, which are in very good agreement with the simulations ones (the black and red solid lines in Fig. 4c). We observe that the cut-off frequency

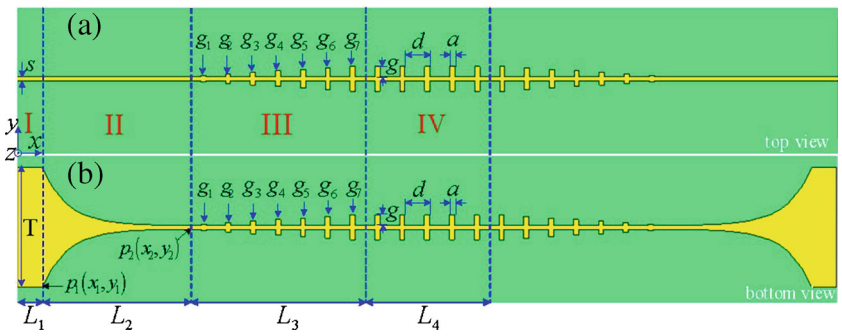

Fig. 3 Schematic pictures of the proposed two-stage back-to-back transitions from the microstrip line to the double-layered CSPW **a** the top view and **b** the bottom view

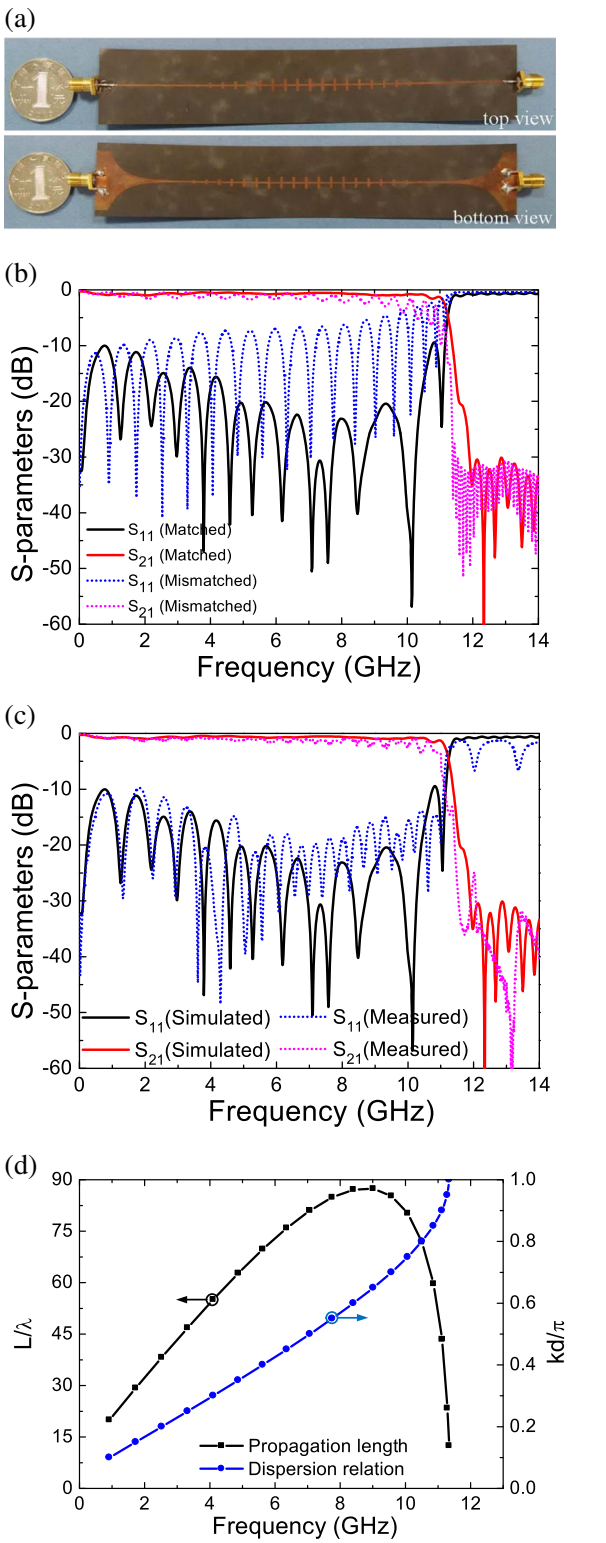

Fig. 4 **a** The photo of the fabricated straight sample (Up: the top view, Down: the bottom view). **b** The simulated *S*-parameters of the straight sample with and without the matching transition. **c** The simulated and measured *S*-parameters of the fabricated straight sample with the matching transition. **d** The normalized propagation length (the black line) and the corresponding dispersion curve (the blue line) of the fundamental surface mode of the double-layered CSPs

is 11.4 GHz in both simulation and measurement, satisfying the dispersion result analyzed in Fig. 2a approximately. In addition, the normalized propagation length (L/λ) of the double-layered CSPs propagating along the proposed double-layered CSPW is calculated and shown in Fig. 4d, in which $L=1/(2\mathrm{Im}(k))$ and $\mathrm{Im}(k)$ is the imaginary part of the complex propagation constant calculated by commercial software COMSOL Multiphysics with the actual dielectric function of copper [12, 21]. We can observe that when the working frequency is approaching the asymptotic frequency, the propagation lengths decrease rapidly, which is consistent with the dispersion property shown as the blue line in Fig. 4d. Specifically, the propagation length is from 20 to 87 wavelengths in the whole operating band, which shows the propagation loss of the proposed CSPW is relatively low at the transmission band. These unique properties show that the proposed two-stage transitions can effectively convert quasi-TEM wave to double-layered CSPs and the whole structure has excellent low-pass filtering performance in broadband with the cutoff frequency easily tuned by typical geometrical parameters of the double-layered SMGs.

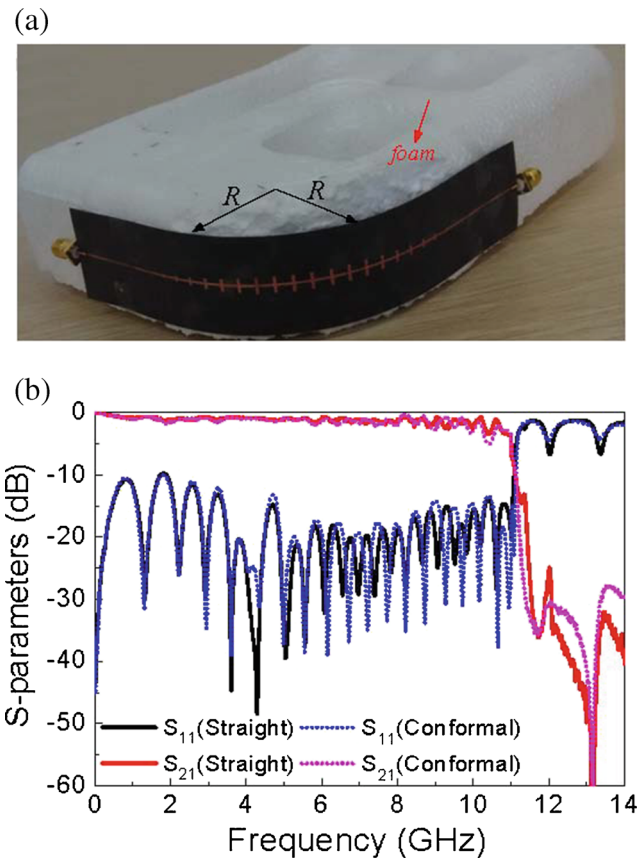

Fig. 5 **a** The photo of the conformal bending sample. **b** The measured *S*-parameters of the fabricated conformal bending and straight samples

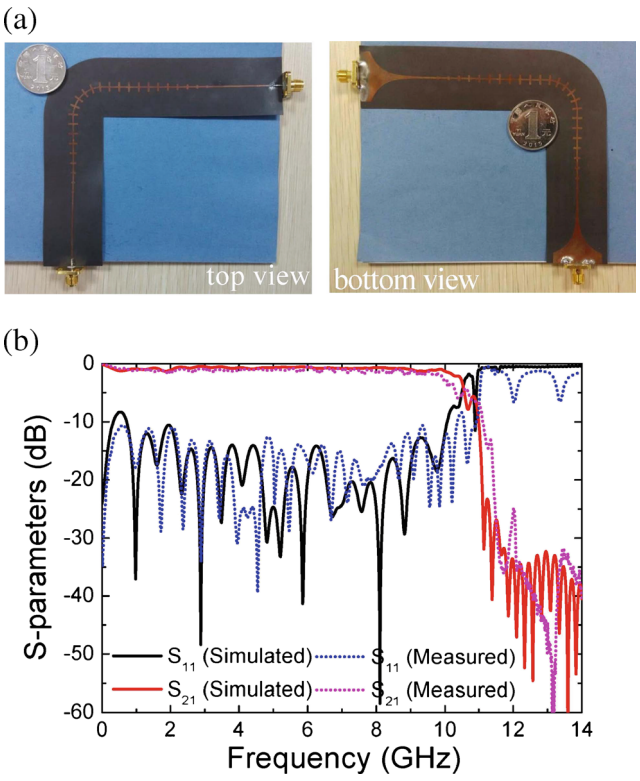

Fig. 6 **a** The photo of the 90^o bending sample (Left: the top view, Right: the bottom view). **b** The simulated and measured *S*-parameters of the 90^o bending sample

It is known that the CSPs can be tightly confined to the ultrathin corrugated metallic strip on arbitrarily curved surfaces. They can travel long distances with very low absorption and radiation losses when the surface is bent, folded, and even twisted [6]. To test the conformal characteristic of double-layered CSPs, the whole structure is fabricated on both sides of a very thin substrate with thickness h = 0.254 mm, which can also be bent and twisted. We first attach the structure to a semi-circle foam board with the radius R = 30 mm exhibited in Fig. 5a, in which all geometrical parameters remain unaltered as that in Fig. 4a. Figure 5b shows the comparison of the measured *S*-parameters results with and without bending, which exhibits little difference in circuit performance. Furthermore, we also expect to test how the propagation of the double-layered CSPs is affected by the presence of a 90^o curved waveguide exhibited in Fig. 6a with the same geometrical parameters as those in Figs. 3 and 4a. As shown in Fig. 6b, the S_{21} is more than -0.9 dB and the S_{11} is less than -10 dB in the frequency range from 0 to 10 GHz. The simulation results are in good agreements with the experiments except the little deviation at high frequencies. These deviations may be caused by the tolerance of fabrication especially in the curved zone, which will cause the impedance mismatch in the curved zone. Moreover, the samples are easily bendable due to the ultrathin geometries, which would cause some discrepancies during the testing process. The scaling-down geometry has great promise to realize high-efficiency plasmonic waveguide in the THz regime.

Conclusions

In summary, we have numerically and experimentally verified an efficient design to achieve mode conversion between the quasi-TEM waves in the common microstrip line and the CSPs on a double-layered CSPW using a two-stage back-to-back transition structure. The simulation and measurement results on the *S*-parameters at microwave frequencies demonstrate excellent circuit performance of the straight and curved double-layered CSPWs. These results could contribute to developing advanced plasmonic integrated circuits in the microwave and THz frequencies.

Acknowledgments This work was supported in part by the Foundation of State Key Laboratory of Millimeter Waves, Southeast University, China, under Grant No. K201603, in part by the Natural Science Foundation of Jiangsu Province under Grant No. BK20151480, in part by the Fundamental Research Funds for the Central Universities under Grant No. NS2016039, in part by the China Scholarship Council, in part by the Funding for Outstanding Doctoral Dissertation in NUAA under Grant No. BCXJ15−04 and in part by the priority academic program development of Jiangsu Higher Education Institutions.

References

1. Pendry JB, Martin-Moreno L, Garcia-Vidal FJ (2004) Mimicking surface plasmons with structured surfaces. Science 305:847–848
2. Garcia-Vidal FJ, Martin-Moreno L, Pendry JB (2005) Surfaces with holes in them: new plasmonic metamaterials. J Opt A-Pure Appl Opt 7:S97–S100
3. Hibbins P, Evans BR, Sambles JR (2005) Experimental verification of designer surface palsmons. Science 308:670–672
4. Barnes WL, Dereux A, Ebbesen TW (2003) Surface plasmon subwavelength optics. Nature 424:824–830
5. Ebbesen TW, Genet C, Bozhevolnyi SI (2008) Surface-plasmon circuitry. Phys Today 61:44
6. Shen X, Cui TJ, Martin-Cano D, Garcia-Vidal FJ (2013) Conformal surface plasmons propagating on ultrathin and flexible films. Proc Natl Acad Sci USA 110:40–45
7. Ma HF, Shen XP, Cheng Q, Jiang WX, Cui TJ (2013) Broadband and high-efficiency conversion from guided waves to spoof surface plasmon polaritons. Laser Photon Rev 10:00118
8. Pan BC, Liao Z, Zhao J, Cui TJ (2014) Controlling rejections of spoof surface plasmon polaritons using metamaterial particles. Opt Express 22:13940
9. Liu LL, Li Z, Gu CQ, Ning PP, Xu BZ, Niu ZY, Zhao YJ (2014) Multi-channel composite spoof surface plasmon polaritons propagating along periodically corrugated metallic thin films. J Appl Phys 116:013501
10. Liao Z, Zhao J, Pan BC, Shen XP, Cui TJ (2014) Broadband transition between microstrip line and conformal surface plasmon waveguide. J Phys D: Appl Phys 47:315103

11. Zhang HC, Liu S, Shen XP, Chen LH, Li LM, Cui TJ (2015) Broadband amplification of spoof surface plasmon polaritons at microwave frequencies. Laser Photon Rev 9:83–90
12. Liu LL, Li Z, Xu BZ, Ning PP, Chen C, Xu J, Chen XL, Gu CQ (2015) Dual-band trapping of spoof surface plasmon polaritons and negative group velocity realization through microstrip line with gradient holes. Appl Phys Lett 107:201602
13. Liao Z, Shen XP, Pan BC, Zhao J, Luo Y, Cui TJ (2015) Combined system for efficient excitation and capture of LSP resonances and flexible control of SPP transmissions. ACS Photon 2:738–743
14. Gao X, Zhou L, Liao Z, Ma HF, Cui TJ (2014) An ultra-wideband surface plasmonic filter in microwave frequency. Appl Phys Lett 104:191603
15. Zhou YJ, Yang BJ (2015) Planar spoof plasmonic ultra-wideband filter based on low-loss and compact terahertz waveguide corrugated with dumbbell grooves. Appl Opt 54:4529–4533
16. Gao X, Zhou L, Cui TJ (2015) Odd-Mode Surface plasmon polaritons supported by complementary plasmonic metamaterial. Sci Rep 5:9250
17. Liu LL, Li Z, Gu CQ, Xu BZ, Ning PP, Chen C, Yan J, Niu ZY, Zhao YJ (2015) Smooth bridge between guided waves and spoof surface plasmon polaritons. Opt Lett 40:8
18. Liu LL, Li Z, Xu BZ, Gu CQ, Chen C, Ning PP, Yan J, Chen XY (2015) High-efficiency transition between rectangular waveguide and domino plasmonic waveguide. AIP Adv 5:027105
19. Kim SG, Chang K (2004) Ultrawide-Band Transitions and new microwave components using Double-Sided Parallel-Strip lines. IEEE Trans Microw Theory Tech 52:2148–2152
20. Smith DR, Vier DC, Koschny T. h., Soukoulis CM (2005) Electromagnetic parameter retrieval from inhomogeneous metamaterials. Phys Rev E 71:036617
21. Ordal MA et al (1983) Optical properties of the metals Al, Co, Cu, Au, Fe, Pb, Ni, Pd, Pt, Ag, Ti, and W in the infrared and far infrared. Appl. Opt. 22:1099–1119